Periodic creation of polar cap patches from auroral transients in the cusp

K. Hosokawa[1,2], S. Taguchi[3], and Y. Ogawa[4,5]

[1] Dept. of Comm. Eng. and Informatics, Univ. of Electro-Communications, Tokyo, Japan
[2] Center for Space Science and Radio Engineering, Univ. of Electro-Communications, Tokyo, Japan
[3] Dept. of Geophysics, Kyoto Univ., Kyoto, Japan
[4] National Institute of Polar Research, Tokyo, Japan
[5] The Graduate Univ. for Advanced Studies (SOKENDAI), Kanagawa, Japan

Correspondence

Keisuke Hosokawa
Department of Communication Engineering and Informatics
University of Electro-Communications, Tokyo 182-8585, Japan

Tel: +81 424 43 5299
Fax: +81 424 43 5293
keisuke.hosokawa@uec.ac.jp

For submission to *Journal of Geophysical Research - Space Physics*

Abstract. On 24 November 2012, an interval of polar cap patches was observed by an all-sky airglow imager located near the dayside cusp. During the interval, the successive appearance of poleward-moving auroral forms (PMAF) was detected, which are known to represent ionospheric manifestations of pulsed magnetic reconnections at the equatorial magnetopause. All of the patches observed during the interval appeared from transient auroral features (i.e., there was a one-to-one correspondence between PMAF and newly-created baby patches). This fact strongly suggests that patches can be directly and seamlessly created from a series of PMAF. The optical intensities of the baby patches were 100–150 R, which is slightly lower than typical patch luminosity on the nightside, and may imply that PMAF-induced patches are generally low-density. The generation of such patches could be explained by impact ionization due to soft particle precipitation into PMAF traces. In spite of the faint signature of the baby patches, two coherent high frequency (HF) radars of the SuperDARN network observed backscatter echoes in the central polar cap, which represented manifestations of plasma irregularities associated with the baby patches. These indicate that patches created from PMAF have the potential to affect the satellite communications environment in the central polar cap region.

Introduction

Polar cap patches are defined as regions of increased plasma density traveling across the polar cap ionosphere [*Crowley*, 1996]. They are believed to be created near the dayside cusp region, and are subsequently transported towards the auroral region on the nightside [*Oksavik et al.*, 2010]. Since their discovery in 1980s, [*Weber et al.*, 1984] patches have been studied using ground-based radio observations [*Pedersen et al.*, 2000; *Milan et al.*, 2002; *McDougall and Jayachandran*, 2007] and in-situ measurements by low-Earth orbiting satellites [*Coley and Heelis*, 1995; *Kivanc and Heelis*, 1997]. In recent years, all-sky airglow imagers (ASIs) equipped with cooled charge-couple (CCD) detectors have been used extensively for capturing the dynamic characteristics of patches [*Hosokawa et al.*, 2006, 2010; Dahlgren et al., 2012a, 2012b]. A significant advantage of airglow measurements is their ability to observe the spatial distribution of patches in a 2D fashion, and with a wide field-of view [e.g., *Hosokawa et al.*, 2014]. Furthermore, the recent use of highly sensitive electron multiplier charge-coupled device (EMCCD) imagers has made it possible to visualize fine-scale structures with improved temporal and spatial resolutions [*Hosokawa et al.*, 2013a; 2013b].

Recent high-quality airglow measurements have greatly contributed to a better understanding of the processes determining the spatial distribution of patches during their long-distance travel across the central polar cap. However, our understanding of patch creation processes remains insufficient. A number of processes have been considered to explain the generation of patches on the dayside [*Carlson*, 2012]: 1) the large-scale reorientation of plasma convection near the cusp due to changes in the interplanetary magnetic field (IMF) B_y and B_z [*Anderson et al.*, 1988; *Sojka et al.*, 1993]; 2) plasma reduction due to convection jets through frictional heating [*Rodger et al.*, 1994; *Valladares et al.*, 1994, 1996]; 3) the capturing of dense plasma in the sunlit region due to the expansion/contraction of the open/closed field line boundary by transient reconnection [*Lockwood and Carlson*, 1992; *Carlson et al.*, 2004, 2006]; and 4) localized plasma enhancement through impact ionization due to cusp precipitation [*Walker et al.*, 1999; *Smith et al.*, 2000; *Oksavik et al.*, 2006]. However, it is still unclear as to which of these mechanisms is dominant.

Recent 630.0 nm airglow measurements in the polar cap have revealed two key characteristics of patches that should be taken into account when discussing patch generation processes: 1) the "cigar-shaped structure" of patches observed by *Hosokawa et al.* [2014], who combined data from two airglow imagers in the polar cap to show that the dawn-dusk extent of patches was more than 1000 km, while the thickness in the noon–midnight direction was less than 500 km, meaning that patches are more elongated in the direction perpendicular to their motion (i.e., their structure is cigar-shaped); 2) patch "periodicity", observed using a highly sensitive EMCCD ASI on the nightside. *Hosokawa et al.* [2013a] found a 5–12 min periodic oscillation in a time-series of patch luminosity, which implies that patches generally have some sort of periodicity. Any proposed patch generation processes must reproduce these two characteristics; therefore, any process that can create cigar-shaped patches in a periodic manner should be considered a strong candidate for the origin of polar cap patches.

Many previous observations have detected periodic aurora phenomena near the dayside cusp region, which are known as poleward moving auroral forms (PMAF) [e.g., *Fasel*, 1995]. PMAF are characterized by 630.0 nm auroral arcs that are detached from the dayside auroral oval and propagate poleward in a periodic manner. It is now widely accepted that PMAF are ionospheric manifestations of pulsed magnetic reconnections at the equatorial magnetopause [e.g., *Wild et al.*, 2001]. *Fasel* [1995] investigated the periodicity of PMAF using a large volume of optical data from the dayside cusp and demonstrated that the typical period of PMAF ranges from a few minutes to 10 min. This periodicity is very similar to that of patches identified on the nightside [*Hosokawa et al.*, 2013a]. Furthermore, the spatial structure of PMAF is known to be more elongated in the longitudinal direction (i.e., in the direction perpendicular to their poleward motion) [e.g., *Milan et al.*, 2000], which is consistent with the cigar-shaped structure of the patches captured in the central polar cap [*Hosokawa et al.*, 2014]. Taking these two similarities into account, it is natural to speculate that patches are directly created from PMAF near the dayside cusp region.

Lorentzen et al. [2010] first validated this theory by investigating the connection between optical signatures of patches and PMAF captured by several optical instruments in Longyearbyen, Norway. In Longyearbyen, daytime aurorae can be observed using ground-based optical instruments for a limited period near the winter solstice. By using data from such unique occasions, *Lorentzen et al.* [2010] showed slight indications of faint airglow features (i.e., signatures of newly-created baby patches) emerging from the poleward moving PMAF traces. Furthermore, they proposed a model of patch generation based on a combination of photoionization, cusp particle precipitation, and the vertical transport of plasma due to heating. However, in their study, the sensitivity of the optical instruments was not optimized for tracking the propagation of baby patches deep into the central polar cap region after their birth in the cusp region. This was primarily because PMAF are generally very bright, up to a few thousand Rayleigh (kR), while the airglow intensity of polar cap patches is normally just a few hundred R. This significant contrast made it impossible to observe these two features simultaneously using a single optical instrument.

The primary objective of this study was to simultaneously observe PMAF and patches in order to visualize how patches are created from PMAF and how they then progress towards the pole. For this purpose, we have operated an EMCCD airglow imager in Longyearbyen, Norway [*Taguchi et al.*, 2012] since October 2012. We have observed both PMAF and patches at 630.0 nm near-simultaneously by splitting our shots into two channels: one with a shorter exposure time (1 s) for observing brighter PMAF, and the other with a longer exposure time (4 s) for detecting the faint airglow enhancement associated with patches. We alternate these two measurements in order to observe bright PMAF and faint airglow patches almost simultaneously. In this manuscript, we show a patch interval that was clearly observed in the longer exposure time data, and examine its connection with PMAF, which were observed in the shorter exposure time data. By investigating such an unique interval, we are able to discuss the generation mechanism of patches in close association with transient auroral phenomena in the cusp region.

Experimental Arrangement

The ASI used in this study has been operative in Longyearbyen, Norway (78.2°N, 15.6°E; AACGM latitude 75.3°) since October 2011 [*Taguchi et al.*, 2012]. It is equipped with an EMCCD camera (Hamamatsu, C9100-13) whose imaging part has 512×512 pixels. The details of the ASI system are provided in *Taguchi et al.* [2012] and recent examples of the polar cap patch observations were introduced in *Hosokawa et al.* [2013a, 2013b]. Since its deployment in 2011, the ASI has observed 630.0 nm airglow images with an exposure time of 4 s in order to detect the airglow signatures of polar cap patches. Since October 2012, in order to observe bright PMAF near the cusp on the dayside, we have taken additional 1-s exposure time 630.0 nm images three times a minute. In addition to the on-going 4-s exposure time measurements, we can now observe the 630.0 nm airglow using different exposure times quasi-simultaneously.

In order to see how patches are transported deep into the dark polar cap ionosphere after their birth in the cusp, we have made use of two SuperDARN radars at Rankin Inlet (62.82°N, 93.11°W; AACGM latitude 72.96°) and Inuvik (62.82°N, 93.11°W; AACGM latitude 72.96°), which form part of the international SuperDARN network [*Chisham et al.*, 2007]. The coherent high frequency (HF) radars of the SuperDARN network are able to observe backscatter echoes from decameter-scale field-aligned irregularities associated with polar cap patches, which are known to distribute throughout patches [*Hosokawa et al.*, 2009]. Thus, the spatial distribution of radar backscatter echoes can be used as proxies for patches in the central polar cap region.

On 24 November 2012 (the day of the present observations), the radars were operating in a special scan mode, in which measurements were made only along 3 beams that were binned into 75 range gates (with a separation between the gates of 45 km).

Observations

During a 4-h interval from 0500 to 0900 UT on November 24, 2012, the ASI in Longyearbyen observed successive appearance and subsequent poleward progression of PMAF in the vicinity of the dayside cusp. Figure 1a shows 630.0 nm optical data taken with an exposure time of 1 s in a keogram format (i.e., a time vs. zenith angle plot of the optical intensity reproduced from consecutive ASI images). Here, the keogram is along the south–north cross section, which is suitable for demonstrating the poleward development of PMAF. Throughout the interval, a continuous band of 630.0 nm aurora was observed mainly in the southern half of the field-of-view (FOV). The equatorward edge of this band was believed to be the signature of the open/closed field-line boundary (OCB). A number of poleward moving bright traces observed in the keogram were manifestations of PMAF. They first appeared from the OCB, moved poleward towards the zenith, and eventually disappeared somewhere in the northern half of the FOV, which is typical of a PMAF signature [e.g., *Fasel et al.*, 1995]. During the first half of the interval, the OCB was located far south of Longyearbyen, which is favorable for capturing patch creation in the central part of the FOV. Thus, we hereafter focus on the 1-h interval from 0545 to 0645 UT (Figure 1a).

In the bottom four panels of Figure 1, the IMF B_y, IMF B_z, solar wind proton density, and solar wind velocity during the interval of PMAF are displayed. These parameters were obtained by the Advanced Composition Explorer (ACE) spacecraft located far upstream of the Earth (X_{GSM} ∼222 R_e). As shown in Figure 1e, the solar wind speed ranged from 350 to 380 km s^{-1}, with a mean of around 370 km s^{-1}. Figure 1d shows that the solar wind proton density was very variable; however, the mean density was $\sim$11 cc^{-1}. By using these parameters, we estimated the delay time of the solar wind from the spacecraft position to the dayside cusp ionosphere to be $\sim$71 min, following a method proposed by *Khan and Cowley* [1999]. The time-series in the bottom four panels of Figure 1 have been shifted accordingly. The IMF B_z in Figure 1c was predominantly negative during the interval, with just several excursions to positive. Hence, the high-latitude ionosphere should have been dominated by a twin-cell convection pattern [e.g., *Ruohoniemi et al.*, 2005], which is a suitable situation for the appearance of both PMAF [*Fasel et al.*, 1995] and patches [*Hosokawa et al.*, 2009b]. The IMF B_y in Figure 1b was positive almost throughout this interval. In such a situation, the flow near the cusp is typically directed from dusk to dawn due to the magnetic tension force applied by the magnetic reconnection at the dayside magnetopause [*Cowley et al.*, 1991].

Figure 2a shows a keogram reproduced from 1-s exposure time images during a 1-h period from 0545 to 0645 UT. During this 1-h interval, the OCB was located far south of Longyearbyen; thus, the evolution of PMAF into patches was captured in the central part of the FOV. In the keogram, there are a number of clear PMAF traces that move poleward repeatedly. They are considered to represent signatures of pulsed equatorial magnetopause reconnection because the IMF B_z was directed southward. During this 1-h interval, we observed nine PMAF signatures (Figure 2b), and although their luminosity changed as they progressed poleward, their optical intensities were a few thousand R. The PMAF repetition period was 4–10 min. Importantly, we only observed bright PMAF signatures in the bottom half of the FOV, but no airglow enhancements associated with newly-created baby patches, which was consistent with the 1-s exposure time.

The 630.0 nm images with a 4-s exposure time were used to observe the signatures of baby patches. The 4-s exposure time data enabled the detection of faint airglow signatures since the signal to noise ratio was better than that of the 1-s exposure time data by a factor of 2. Figure 2c shows the 4-s exposure time data in the format of a S–N keogram. The optical data saturated in the bottom half of the FOV (i.e., in the region of PMAF) because the optical intensity of the PMAF (a few kR) were beyond the dynamic range of the measurements. In contrast, in the poleward half of the FOV, very faint traces are seen to drift poleward, representing the possible signatures of baby patches newly-created from the PMAF. We traced these poleward moving airglow features during the 1-h interval, with a total of 10 poleward moving airglow traces observed (Figure 2d). The 4-s exposure time data well demonstrate that diffuse structures with weak 630.0 nm airglow enhancements existed in the region poleward of PMAF and drifted further poleward toward the central polar cap region (Figures 2c and 2d).

To confirm the connection between the PMAF and baby patches, we plotted the observed PMAF traces and patches as a function of time and magnetic latitude (Figure 3). We observed a one-to-one correspondence between the PMAF in the shorter exposure time data and the baby airglow patches in the longer exposure time data; although, the first baby patch did not have a counterpart in the PMAF observations. Namely, the connection between PMAF and baby patches was seamless, providing evidence for the direct creation of patches from PMAF. Furthermore, the airglow signatures of the baby patches reached at least 80° in the altitude adjustment corrected geomagnetic (AACGM) magnetic latitudes [*Baker and Wing*, 1989], which meant that the patches created from the PMAF did not disappear soon after initiation, but were transported long distances into the central polar cap. The generation and subsequent poleward progression of such newly created patches is more clearly seen in 2D animation (Animation 1).

In order to investigate the changing luminosity of baby patches during their poleward development, we plotted the optical intensity of several points in the keogram (Figure 4a) as a time-series (Figure 4b). Several peaks maintained their intensity during poleward propagation, which is consistent with the baby patch signatures traveling towards the central polar cap. The optical intensity of these baby patches was at least 100–150 R above the background level, roughly consistent with the optical intensity of patches on the nightside. However, patches observed on the nightside often show an optical intensity of a few hundred R, even after their long distance travel from the dayside [e.g., *Hosokawa et al.*, 2006]. This means that the optical intensity of the baby patches during the current interval was slightly smaller than that in typical cases; thus, the patches during the current interval might be categorized as low-density [e.g., *Zhang et al.*, 2013].

Figure 5 shows a snapshot of a 4-s exposure time 630.0 nm image taken at 0630 UT, which has been mapped onto the magnetic latitude and magnetic local time (MLT) coordinate system. At around 9–10 MLT, the FOV of the ASI was located near the cusp. The image shows the faint airglow signatures of baby patches in the poleward half of the FOV. Superimposed on the ASI image are contours of the electrostatic potential derived from all of the northern hemisphere SuperDARN radars using an algorithm developed by *Ruohoniemi and Baker* [1998]. The potential contours show a stream extending from the vicinity of the FOV towards the nightside auroral region and all the way across the central polar cap region. The beam directions of the SuperDARN Rankin Inlet and Inuvik radars (Figure 5) well cover the possible trajectories of the patches produced on the dayside. In past studies, many authors have used the coherent HF radars of the SuperDARN network to demonstrate that polar cap patches are detectable as blobs of irregularities [e.g., *Milan et al.*, 2002]. In particular, *Hosokawa et al.* [2009a] reported irregularities distributed in the entire region of airglow patches. This allows us to observe the transportation of the polar cap patches using the data from the two SuperDARN radars.

The data from the two SuperDARN radars show a number of blobs in radar echoes whose backscatter power is significantly greater than 30 dB (Figure 6). Since the radars were located on the nightside and the beams pointed towards the dayside, these irregularities, which moved towards the radars, corresponded to the anti-sunward moving polar cap patches. The Doppler velocities from these echo regions were mostly positive, which is also consistent with a velocity toward the radar. Thus, the radar patches were actually moving anti-sunward, away from their source in the vicinity of the cusp region. During the interval of interest, only three beams were operative for both of the SuperDARN radars (Animation 1). Although the number of beams was not enough to visualize the motion of irregularities in a 2D fashion, there were some indications of the anti-sunward transport of patches along the three beams. This indicates that the patches reached the nightside polar cap, and that there existed small-scale irregularities in the polar cap, despite the low density of the patches.

Discussion

As discussed, patches observed on the nightside show two key characteristics: a "cigar-shaped structure" [*Hosokawa et al.*, 2014] and "5–12 min periodicity" [*Hosokawa et al.*, 2013a]. Our results show that patches were created from PMAF periodically (Figures 2c and 2d) and that the repetition period of the PMAF was 4–10 min, which mirrored that of the newly-created patches. Thus, the patches created during the present interval had periodicity consistent with *Hosokawa et al.* [2013a]. Furthermore, PMAF were more elongated in the east–west direction (i.e., in the direction perpendicular to their poleward motion; Animation 1). Since the patches were created directly from the PMAF, they also had a similar spatial structures extending more toward the east–west direction. If these baby patches were transported toward the central polar cap, their structures should have been more elongated in the dawn-dusk direction, consistent with the cigar-shaped structure of patches introduced by *Hosokawa et al.* [2014]. Thus, our results support the direct creation of patches from PMAF, with a certain fraction of the patches detected on the nightside originating from periodic poleward motion of PMAF in the dayside cusp, which was first implied by *Lorentzen et al.* [2010]. Recently, *Dahlgren et al.* [2012a, 2012b] showed that weak airglow patches observed in the polar cap had a possible connection with 4–8 min periodic auroral behavior on the dayside, which can also be explained by the direct generation of patches from PMAF near the cusp.

Lockwood and Carlson [1992] proposed a model for the patch generation mechanism based on transient reconnection on the dayside. In their model, the transient expansion/contraction of OCB due to pulsed reconnection [*Cowley and Lockwood*, 1992] captures low-latitude high density plasma as patches. This model was tested by *Carlson et al.* [2004, 2006], and remains one of the most widely accepted mechanisms of patch generation. Since PMAF are known as signatures of pulsed reconnection at the equatorial magnetopause, the *Lockwood and Carlson* [1992] model could explain the direct connection between PMAF and patches seen in the current study. The suggested expanding/contracting motion of OCB can capture the solar-produced high density plasma located equatorward of the cusp. However, such a shift in OCB is known to be $\sim 2°$ [*Greenwald et al.*, 1999; *Chisham et al.*, 2001]; thus, the plasma captured by the transient equatorward leap of the boundary may not be sufficient for the production of dense F region patches. In addition, *Lorentzen et al.* [2010] reported no signature of the equatorward leap of OCB, which is consistent with our study, as we were also not able to identify signatures of large-scale equatorward leap in the keograms (Figure 1a and 2a). More recently, *Goodwin et al.* [2015] showed that by using successive over flights of the Swarm satellite through the dayside cusp, the solar extreme ultraviolet (EUV) plasma in the subauroral region could be clearly separated from cusp precipitation. By considering these observational facts, the generation of patches from PMAF cannot be explained solely by the model of *Lockwood and Carlson* [1992].

Another process possibly contributing to the generation of patches is impact ionization due to particle precipitation into PMAF. The generation of patches by particle precipitation was first suggested by *Walker et al.* [1999], who combined optical observations with radio tomography to show that precipitation of soft particles into the cusp can create substantial ionization above 250 km altitude, which is consistent with the process of in-situ patch creation due to precipitation. *Smith et al.* [2000] presented a case in which polar cap patches are created by repetitive intensifications of soft-particle precipitation into the cusp, possibly associated with transient reconnections at the magnetopause. A similar conclusion was obtained by *Goodwin et al.* [2015], who employed data from successive over flights of the Swarm satellite through the dayside cusp to investigate the role played by particle precipitation on the creation of patches. In this study, there was an exact one-to-one correspondence between PMAF and patches, which implies that the patches were directly produced through soft particle precipitation into the traces of PMAF. *Millward et al.* [1999] estimated how electron density in the F region is enhanced due to particle impact ionization in the cusp. Their model suggests that the production rate of ionization at 300 km altitude is $\sim 8 \times 10^8$ m^{-3}s^{-1} in the cusp. The lifetime of PMAF observed in this study (Figure 2a) was about 5 min; thus, we could expect an increase in the electron density of 2–3$\times 10^{11}$ m^{-3}. Based on the model of *Sakai et al.* [2014], who investigated the relationship between 630.0 nm airglow intensity and F region peak density, an electron density of 2–3$\times 10^{11}$ m^{-3} roughly corresponds to an airglow intensity of 100–200 R. This value is consistent with the observed airglow intensities of the newly-created baby patches (Figure 4b), which suggests that the soft particle precipitation into PMAF can create patches without any horizontal transport of solar EUV plasma from the low-latitude region.

However, even though the observed optical intensity of the newly-created patches can be explained by soft particle precipitation into PMAF, it remains unclear whether such precipitation-induced patches are able to survive for a long time during their travel towards the nightside. The airglow intensity of polar cap patches observed on the nightside is often a few hundred R [e.g., *Hosokawa et al.*, 2006, 2009b]. In contrast, the airglow intensity of the newly-created patches (Figure 4c) was up to 150 R. This implies that the patches in the current interval should be categorized as low-density. In some previous studies, high- and low-density patches have been treated separately. For example, *Zhang et al.* [2013] discussed the generation mechanisms of high- and low-density patches separately and suggested that low-density patches are created by particle precipitation during a series of transient reconnection events. The results of *Zhang et al.* [2013] and those of the current study may mean that patches directly created from PMAF are generally low-density. It has been demonstrated that high-density patches ($>$ 500 R) are often observed on the nightside, some of which are known as the tongue of ionization (TOI: *Foster et al.* [2005], *Hosokawa et al.* [2010]). Such high-density patches should be associated with the horizontal transport of low-latitude plasma; although, the internal structure of high-density patches should be caused by PMAF when it is transported through the cusp inflow region [*Hosokawa et al.*, 2010]. It is clear from the current observations that the patches generated from PMAF should be different from high-density patches and that they may be very weak or invisible when they reach the nightside auroral region.

The two SuperDARN radars detected blobs of irregularities propagating anti-sunward in the central polar cap region. By considering the streamline of high-latitude convection derived from the SuperDARN network, we can see that these blobs were transported from the cusp near the FOV of the ASI in Longyearbyen. The ASI data show that the newly-created patches were low-density (i.e., faint in the airglow data). However, the radar data indicate that these patches were structured enough to produce radar backscatter echoes. This implies that even low-density patches created from PMAF can produce strong radar backscatter echoes in the central polar cap area. These irregularities may cause scintillation effects on the trans-ionospheric satellite link. In past studies, patch-associated irregularities have been attributed to gradient-drift instability [*Gondarenko and Guzdar*, 2006 and references therein]. However, more recently, *Goodwin et al.* [2015] used electron density observations from the Swarm satellite to show that precipitation in the cusp already has structured patches that become smooth as they travel towards the nightside. Since the patches observed in this study were low-density, structuring through gradient-drift instability may have been difficult; however, we observed strong radar backscatter echoes well after the birth of patches in the cusp, which implies the possible role of particle precipitation in the source region of the structuring of polar cap patches.

Summary and Conclusion

We have shown that an interval of polar cap patches was seamlessly produced from a series of PMAF. *Lorentzen et al.* [2010] also demonstrated this process using optical measurements of PMAF near the cusp. However, in their event, the sensitivity of the optical instruments was not optimized for visualizing the transportation of newly-created patches deep into the central polar cap. In this study, we changed the exposure time shot by shot and obtained images with different sensitivities quasi-simultaneously, making it possible to observe bright PMAF and dim patches at the same time by using a single ASI. As a result, we succeeded in visualizing the generation of patches from PMAF and their subsequent propagation into the polar cap while maintaining their density. The optical intensity of the newly-created patches was 100–150 R, which is slightly lower than that of typical patches observed on the nightside. This may imply that patches created from PMAF are generally lower density. We suggest that the creation of such low-density patches can be explained by in-situ impact ionization due to soft particle precipitation into PMAF; although, the transport of high-density plasma from low-latitudes may contribute to plasma enhancement. In addition to optical measurements on the dayside, we employed data from two SuperDARN radars in the nighttime polar cap and demonstrated that the newly-created patches traveled towards the nightside across the central polar cap area. This observation confirms that polar cap patches on the nightside originate from PMAF in the dayside cusp region. Furthermore, the radar observations suggest plasma irregularities associated with the low-density patches created from PMAF, which may affect the satellite communications environment in the polar cap region.

Acknowledgments. We would like to thank Takeshi Aoki for his continued support in constructing, installing, and maintaining our optical instrument in Longyearbyen. We also thank F. Sigernes for his help at The University Centre in Svalbard, Longyearbyen. The authors wish to thank N. Ness at the Bartol Research Institute for access to data from magnetic field (MFI) and solar wind electron (SWE) instruments onboard the Advanced Composition Explorer (ACE) spacecraft. The authors acknowledge the use of data from the SuperDARN network, a collection of radars funded by national scientific funding agencies of Australia, Canada, China, France, Japan, South Africa, the United Kingdom, and the United States of America. This work was supported by Grants-in-Aid for Scientific Research (22340143 and 26302006) from the Japan Society for the Promotion of Science (JSPS). The ground optical data used in this study can be provided on request to Satoshi Taguchi, Kyoto University. Solar wind data from the ACE spacecraft can be accessed through the ACE science center at http://www.srl.caltech.edu/ACE/ASC/.

References

Anderson, D. N., J. Buchau, and R. A. Heelis (1988), Origin of density enhancements in the winter polar cap ionosphere, *Radio Sci., 23*, 513–519, doi:10.1029/RS023i004p00513.

Baker, K. B., and S. Wing (1989), A new magnetic coordinate system for conjugate studies of high latitudes, *J. Geophys. Res., 94*, 9139.

Carlson, H. C., K. Oksavik, J. Moen, and T. Pedersen (2004), Ionospheric patch formation: Direct measurements of the origin of a polar cap patch, *Geophys. Res. Lett., 31*, doi:10.1029/2003GL018166.

Carlson, H. C., J. Moen, K. Oksavik, C. P. Nielsen, I. W. McCrea, T. R. Pedersen, and P.

Gallop (2006), Direct observations of injection events of subauroral plasma into the polar cap, *Geophys. Res. Lett., 33*, doi:10.1029/2005GL025230.

Carlson, H. C. (2012), Sharpening our thinking about polar cap ionospheric patch morphology, research, and mitigation techniques, *Radio Sci., 47*, doi:10.1029/2011RS004946.

Chisham, G., M. Pinnock, and A. S. Rodger (2001), The response of the HF radar spectral width boundary to a switch in the IMF By direction: Ionospheric consequences of transient dayside reconnection?, *J. Geophys. Res.*, 106, 191–202, doi:10.1029/2000JA900094.

Coley, W. R., and R. A. Heelis (1995), Adaptive identification and characterization of polar ionization patches, *J. Geophys. Res., 100*, 23819–23827, doi:10.1029/95JA02700.

Cowley, S. W. H., J. P. Morelli, and M. Lockwood (1991), Dependence of convective flows and particle precipitation in the high-latitude dayside ionosphere on the X and Y components of the interplanetary magnetic field, *J. Geophys. Res., 96*, 5557–5564, doi:10.1029/90JA02063.

Cowley, S. W. H., and M. Lockwood (1992), Excitation and decay of solar wind-driven flows in the magnetosphere-ionosphere system, *Ann. Geophys., 10*, 103–115, 1992.

Crowley, G. (1996), Critical review of ionospheric patches and blobs, in *Review of Radio Science 1993–1996*, edited by W. R. Stone, Oxford University Press, New York, 619.

Dahlgren, H., J. L. Semeter, K. Hosokawa, M. J. Nicolls, T. W. Butler, M. G. Johnsen, K. Shiokawa, and C. Heinselman (2012a), Direct three-dimensional imaging of polar ionospheric structures with the Resolute Bay Incoherent Scatter Radar, *Geophys. Res. Lett., 39*, doi:10.1029/2012GL050895.

Dahlgren, H., G. Perry, J. Semeter, J.-P. St.-Maurice, K. Hosokawa, M. Nicolls, M. Greffen, K. Shiokawa, and C. Heinselman (2012b), Space-time variability of polar cap patches: direct evidence for internal plasma structuring, *J. Geophys. Res., 117*, doi:10.1029/2012JA017961.

Fasel, G. J. (1995), Dayside poleward moving auroral forms: A statistical study, *J. Geophys. Res., 100*, 11891–11905, doi:10.1029/95JA00854.

Foster, J. C., et al. (2005), Multiradar observations of the polar tongue of ionization, *J. Geophys. Res., 110*, doi:10.1029/2004JA010928.

Goodwin L. V., et al. (2015), Swarm in situ observations of F region polar cap patches created by cusp precipitation, *Geophys. Res. Lett., 42*, doi:10.1002/2014GL062610.

Gondarenko, N. A., and P. N. Guzdar (2006), Nonlinear three-dimensional simulations of mesoscale structuring by multiple drives in high-latitude plasma patches, *J. Geophys. Res., 111*, doi:10.1029/2006JA011701.

Greenwald, R. A., J. M. Ruohoniemi, K. B. Baker, W. A. Bristow, G. J. Sofko, J.-P. Villain, M. Lester, and J. Slavin (1999), Convective response to a transient increase in day-side reconnection, *J. Geophys. Res., 104*, 10,007, 1999.

Hosokawa, K., K. Shiokawa, Y. Otsuka, A. Nakajima, T. Ogawa, and J. D. Kelly (2006), Estimating drift velocity of polar cap patches with all-sky airglow imager at Resolute Bay, Canada, *Geophys. Res. Lett., 33*, 10.1029/2006GL026916.

Hosokawa, K., K. Shiokawa, Y. Otsuka, T. Ogawa, J.-P. St-Maurice, G. J. Sofko, and D. A. Andre (2009a), The relationship between polar cap patches and field-aligned irregularities as observed with an all-sky airglow imager at Resolute Bay and the SuperDARN radar at Rankin Inlet, *J. Geophys. Res., 114*, 10.1029/2008JA013707.

Hosokawa, K., T. Kashimoto, S. Suzuki, K. Shiokawa, Y. Otsuka, and T. Ogawa (2009b), Motion of polar cap patches: A statistical study with all-sky airglow imager at Resolute Bay, Canada, *J. Geophys. Res., 114*, 10.1029/2008JA014020.

Hosokawa, K., T. Tsugawa, K. Shiokawa, Y. Otsuka, N. Nishitani, T. Ogawa, and M. R.

Hairston (2010), Dynamic temporal evolution of polar cap tongue of ionization during magnetic storm, *J. Geophys. Res., 115*, doi:10.1029/2010JA015848.

Hosokawa K., S. Taguchi, Y. Ogawa, and T. Aoki, (2013a), Periodicities of polar cap patches, *J. Geophys. Res., 118*, doi:10.1029/2012JA018165.

Hosokawa, K., S. Taguchi, Y. Ogawa, and J. Sakai (2013b), Two-dimensional direct imaging of structuring of polar cap patches, *J. Geophys. Res., 118*, 6536–6543, doi:10.1002/jgra.50577.

Hosokawa, K., S. Taguchi, K. Shiokawa, Y. Otsuka, Y. Ogawa, and M. Nicolls (2014), Global imaging of polar cap patches with dual airglow imagers, *Geophys. Res. Lett., 41*, 1–6, doi:10.1002/2013GL058748.

Keskinen, M. J., and S. L. Ossakow (1982), Nonlinear evolution of plasma enhancements in the auroral ionosphere 1. long wavelength irregularities, *J. Geophys. Res., 87*, 144.

Khan, H., and S. W. H. Cowley (1999), Observations of the response time of high-latitude ionospheric convection to variations in the interplanetary magnetic field using EISCAT and IMP-8 data, *Ann. Geophys., 17*, 1306.

Kivanc, O., and R. A. Heelis (1997), Structures in ionospheric number density and velocity associated with polar cap ionization patches, *J. Geophys. Res., 102*, doi:10.1029/96JA03141.

Lockwood, M., and H. C. Carlson (1992), Production of polar cap electron density patches by transient magnetopause reconnection, *Geophys. Res. Lett., 19*, doi:10.1029/92GL01993.

Lorentzen, D. A., N. Shumilov, and J. Moen (2004), Drifting airglow patches in relation to tail reconnection, *Geophys. Res. Lett., 31*, L02806, doi:10.1029/2003GL017785.

MacDougall J., and P. T. Jayachandran (2007), Polar patches: Auroral zone precipitation effects, *J. Geophys. Res., 112*, doi:10.1029/2006JA011930.

McEwen, D. J., and D. P. Harris (1996), Occurrence patterns of F layer patches over the north magnetic pole, *Radio Sci., 31*, 619–628.

Milan, S. E., M. Lester, S. W. H. Cowley, and M. Brittnacher (2000), Convection and auroral response to a southward turning of the IMF: Polar UVI, CUTLASS, and IMAGE signatures of transient magnetic flux transfer at the magnetopause, *J. Geophys. Res., 105*, 15741–15755, doi:10.1029/2000JA900022.

Milan, S. E., M. Lester, and T. K. Yeoman (2002), HF radar polar patch formation revisited: summer and winter variations in dayside plasma structuring, *Ann. Geophys., 20*, 487.

Millward, G. H., R. J. Moffett, H. F. Balmforth, and A. S. Rodger (1999), Modeling the ionospheric effects of ion and electron precipitation in the cusp, *J. Geophys. Res., 104*, 24603–24612, doi:10.1029/1999JA900249.

Moen, J., N. Gulbrandsen, D. A. Lorentzen, and H. C. Carlson (2007), On the MLT distribution of F region polar cap patches at night, *Geophys. Res. Lett., 34*, L14113, doi:10.1029/2007GL029632.

Moen, J., K. Oksavik, T. Abe, M. Lester, Y. Saito, T. A. Bekkeng, and K. S. Jacobsen (2012), First in-situ measurements of HF radar echoing targets, *Geophys. Res. Lett., 39*, doi:10.1029/2012GL051407.

Moen, J., K. Oksavik, L. Alfonsi, Y. Daabakk, V. Romano, and L. Spogli (2013), Space weather challenges of the polar cap ionosphere, *J. Space Weather Space Clim., 3*, doi:10.1051/swsc/2013025.

Ogawa, T., S. C. Buchert, N. Nishitani, N. Sato, and M. Lester (2001), Plasma density suppression process around the cusp revealed by simultaneous CUTLASS and EISCAT Svalbard radar observations, *J. Geophys. Res., 106*, 5551.

Oksavik, K., J. M. Ruohoniemi, R. A. Greenwald, J. B. H. Baker, J. Moen, H. C. Carlson, T. K. Yeoman, and M. Lester (2006), Observations of isolated polar cap patches by the

European Incoherent Scatter (EISCAT) Svalbard and Super Dual Auroral Radar Network (SuperDARN) Finland radars, *J. Geophys. Res., 111*, doi:10.1029/2005JA011400.

Oksavik, K., V. L. Barth, J. Moen, and M. Lester (2010), On the entry and transit of high-density plasma across the polar cap, *J. Geophys. Res., 115*, doi:10.1029/2010JA015817.

Ossakow, S. L., and P. K. Chaturvedi (1979), Current convective instability in the diffuse aurora, *Geophys. Res. Lett., 6*, 332–334.

Pedersen, T., B. Fejer, R. Doe, and E. Weber (1998), Incoherent scatter radar observations of horizontal F region plasma structure over Sondrestrom, Greenland, during polar cap patch events, *Radio Sci., 33*, 1847.

Pedersen, T., B. Fejer, R. Doe, and E. Weber (2000), An incoherent scatter radar technique for determining two-dimensional horizontal ionization structure in polar cap F region patches, *J. Geophys. Res., 105*, 10,637.

Prikryl, P., P. T. Jayachandran, S. C. Mushini, and R. Chadwick (2011), Climatology of GPS phase scintillation and HF radar backscatter for the high-latitude ionosphere under solar minimum conditions, *Ann. Geophys., 29*, 377–392, doi:10.5194/angeo-29-377-2011.

Rijnbeek, R. P., S. W. H. Cowley, D. J. Southwood, and C. T. Russell (1984), A survey of dayside flux transfer events observed by ISEE 1 and 2 magnetometers, *J. Geophys. Res., 89*, 786–800, doi:10.1029/JA089iA02p00786.

Rodger, A. S., M. Pinnock, J. R. Dudeney, K. B. Baker, and R. A. Greenwald (1994), A new mechanism for polar patch formation *J. Geophys. Res., 99*, 6425.

Ruohoniemi, J. M., and K. B. Baker (1998), Response of high latitude convection to a sudden southward IMF turning, *Geophys. Res. Lett., 25*, 2913.

Ruohoniemi, J. M., and R. A. Greenwald (2005), Dependencies of high-latitude plasma convection: Consideration of interplanetary magnetic field, seasonal, and universal time factors in statistical patterns, *J. Geophys. Res., 110*, doi:10.1029/2004JA010815.

Sakai, J., K. Hosokawa, S. Taguchi, and Y. Ogawa (2014), Storm time enhancements of 630.0 nm airglow associated with polar cap patches, *J. Geophys. Res., 119*, 2214–2228, doi:10.1002/2013JA019197.

Smith, A. M., S. E. Pryse, and L. Kersley (2000), Polar patches observed by ESR and their possible origin in the cusp region, *Ann. Geophys., 18*, 1043–1053, doi:10.1007/s00585-000-1043-5.

Sojka, J. J., M. D. Bowline, R. W. Schunk, D. T. Decker, C. E. Valladares, R. Sheehan, D. A. Anderson, and R. A. Heelis (1993), Modeling polar cap F-region patches using time varying convection, *Geophys. Res. Lett., 20*, 1783–1786.

Taguchi, S., K. Hosokawa, Y. Ogawa, T. Aoki, and M. Taguchi (2012), Double bursts inside a poleward-moving auroral form in the cusp, *J. Geophys. Res., 117*, doi:10.1029/2012JA018150.

Valladares, C. E., S. Basu, J. Buchau, and E. Friis-Christensen (1994), Experimental evidence for the formation and entry of patches into the polar cap, *Radio Sci., 29*, 167–194, doi:10.1029/93RS01579.

Valladares, C. E., D. T. Decker, R. Sheehan, and D. N. Anderson (1996), Modeling the formation of polar cap patches using large plasma flows, *Radio Sci., 31*, 573–593, doi:10.1029/96RS00481.

Walker, I. K., J. Moen, L. Kersley, and D. A. Lorentzen (1999), On the possible role of cusp/cleft precipitation in the formation of polar-cap patches, *Ann. Geophys., 17*, 1298–1305, doi:10.1007/s00585-999-1298-4.

Weber, E. J., J. Buchau, J. G. Moore, J. R. Sharber, R. C. Livingston, J. D. Winningham, and B. W. Reinisch (1984), F layer ionization patches in the polar caps, *J. Geophys. Res., 89*, 1683.

Wild, J. A., et al. (2001), First simultaneous observations of flux transfer events at the high-latitude magnetopause by the Cluster spacecraft and pulsed radar signatures in the conjugate ionosphere by the CUTLASS and EISCAT radars, *Ann. Geophys., 19* 1491–1508.

Zhang, Q.-H., B.-C. Zhang, J. Moen, M. Lockwood, I. W. McCrea, H.-G. Yang, H.-Q. Hu, R.-Y. Liu, S.-R. Zhang, and M. Lester (2013), Polar cap patch segmentation of the tongue of ionization in the morning convection cell, *Geophys. Res. Lett., 40*, 2918–2922, doi:10.1002/grl.50616.

Figure Captions

Figure 1 (a) Keogram reproduced from 630.0 nm all-sky images along the S–N cross section from 0500 to 0900 UT on 24 November 2012. The horizontal green line denotes the 0545 to 0645 UT focus of this study. (b) Interplanetary magnetic field (IMF) B_y obtained from the Advanced Composition Explorer (ACE) spacecraft. (c) IMF B_z obtained from the ACE spacecraft. (d) Solar wind proton density obtained from the ACE spacecraft. (e) Solar wind speed obtained from the ACE spacecraft. Time-series are shifted by 71 min to account for the solar wind propagation delay from the spacecraft to the dayside polar cap.

Figure 2 (a) S–N keogram reproduced from 1-sec exposure time images between 0545 to 0645 UT on 24 November 2012. (b) Same as (a), but with the signatures of poleward moving auroral forms (PMAF) traced by the red lines. (c) S–N keogram reproduced from 4-sec exposure time images between 0545 to 0645 UT on 24 November 2012. (d) Same as (c), but with the signatures of newly-created patches traced by the blue lines.

Figure 3 Temporal evolution of poleward moving auroral form (PMAF) traces and patches between 0545 to 0645 UT on 24 November 2012.

Figure 4 (a) S–N keogram reproduced from 4-sec exposure time images between 0545 to 0645 UT on 24 November 2012. (b) Temporal variations in the optical intensity at 5 points (Z, and A–D) shown in (a).

Figure 5 Image showing 4-sec exposure time data at 0630 UT mapped onto the magnetic latitude and magnetic local time (MLT) coordinate system. Superimposed blues lines denote electrical potential contours derived from the SuperDARN data. The two green fan-shaped regions show the directions of beam 7 of the SuperDARN Inuvik and Rankin Inlet radars, respectively.

Figure 6 (a) Range-Time-Intensity (RTI) plot showing backscatter power along beam 7 of the SuperDARN Inuvik radar from 0400 to 1200 UT on 24 November 2012. (b) Range-Time-Intensity (RTI) plot showing the line-of-sight Doppler velocity along beam 7 of the SuperDARN Inuvik radar from 0400 to 1200 UT on 24 November 2012. (c) Same as (a), but using data from the SuperDARN Rankin Inlet radar. (d) Same as (b), but using data from the SuperDARN Rankin Inlet radar.

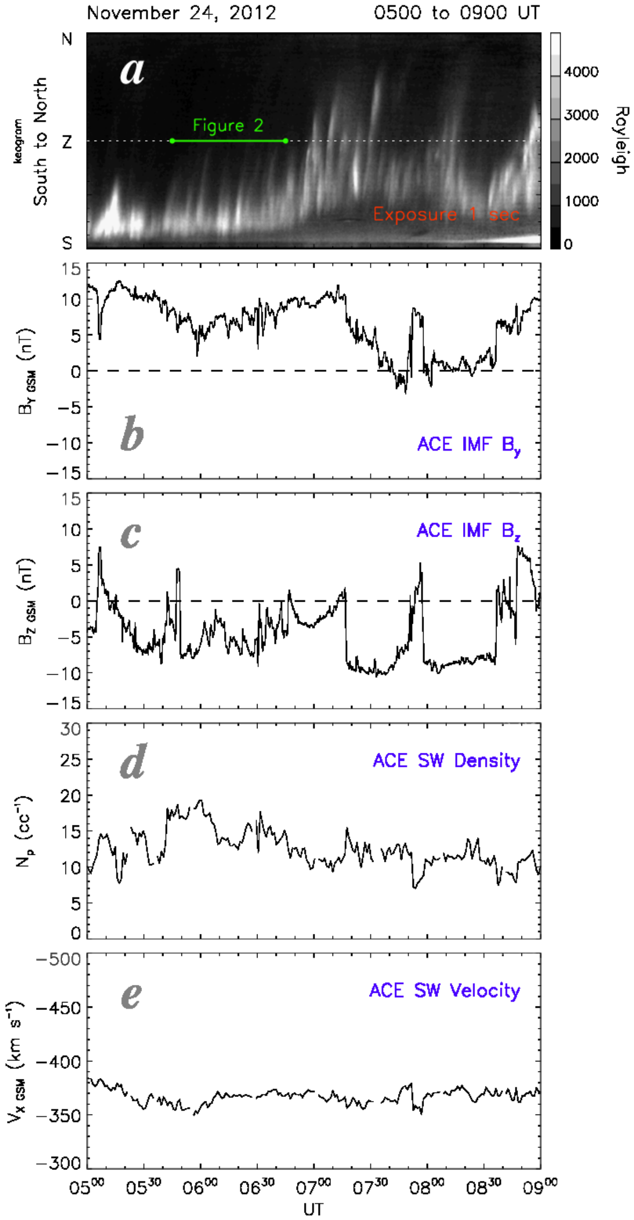

Figure 1 (a) Keogram reproduced from 630.0 nm all-sky images along the S–N cross section from 0500 to 0900 UT on 24 November 2012. The horizontal green line denotes the 0545 to 0645 UT focus of this study. (b) Interplanetary magnetic field (IMF) B_y obtained from the Advanced Composition Explorer (ACE) spacecraft. (c) IMF B_z obtained from the ACE spacecraft. (d) Solar wind proton density obtained from the ACE spacecraft. (e) Solar wind speed obtained from the ACE spacecraft. Time-series are shifted by 71 min to account for the solar wind propagation delay from the spacecraft to the dayside polar cap.

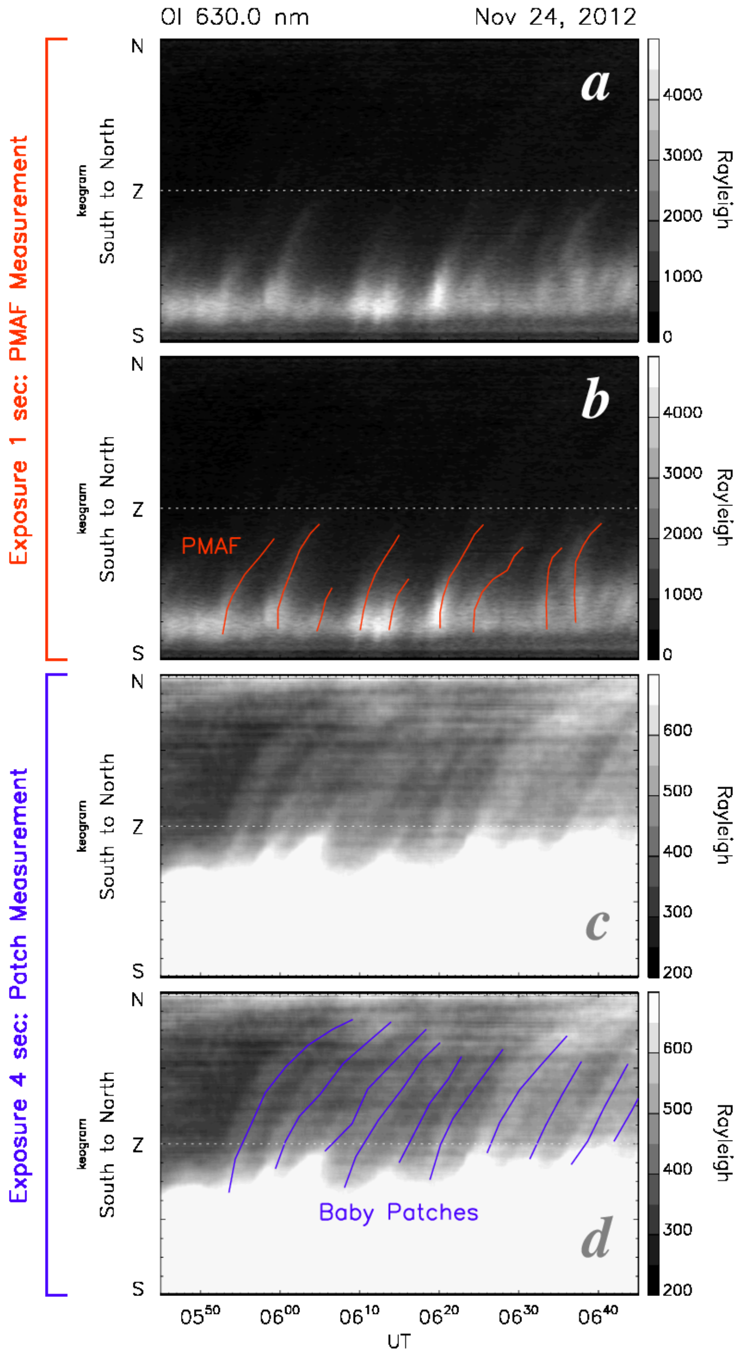

Figure 2 (a) S–N keogram reproduced from 1-sec exposure time images between 0545 to 0645 UT on 24 November 2012. (b) Same as (a), but with the signatures of poleward moving auroral forms (PMAF) traced by the red lines. (c) S–N keogram reproduced from 4-sec exposure time images between 0545 to 0645 UT on 24 November 2012. (d) Same as (c), but with the signatures of newly-created patches traced by the blue lines.

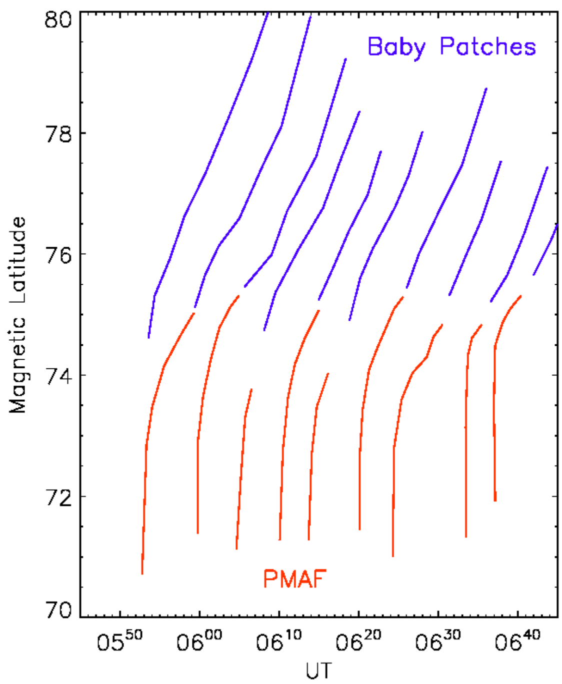

Figure 3 Temporal evolution of poleward moving auroral form (PMAF) traces and patches between 0545 to 0645 UT on 24 November 2012.

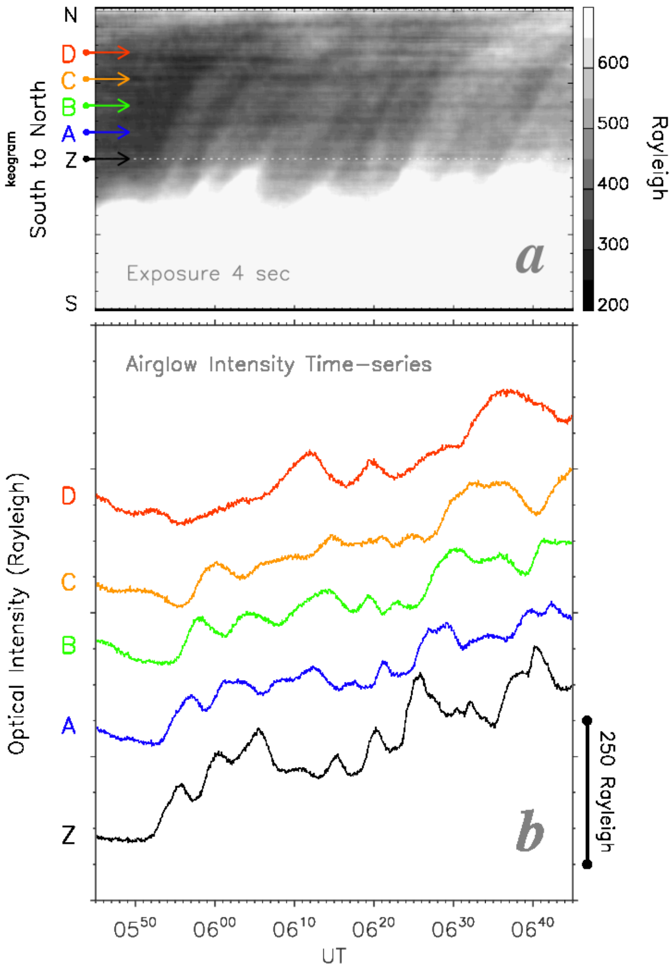

Figure 4 (a) S–N keogram reproduced from 4-sec exposure time images between 0545 to 0645 UT on 24 November 2012. (b) Temporal variations in the optical intensity at 5 points (Z, and A–D) shown in (a).

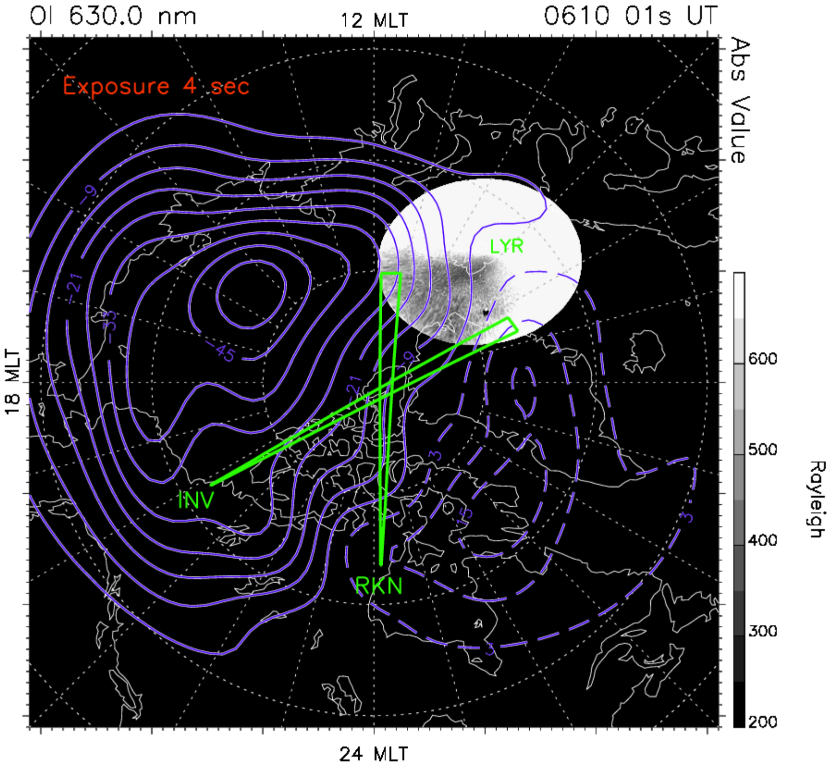

Figure 5 Image showing the 4-sec exposure time data at 0630 UT mapped onto the magnetic latitude and magnetic local time (MLT) coordinate system. Superimposed blues lines denote electrical potential contours derived from the SuperDARN data. The two green fan-shaped regions show the directions of beam 7 of the SuperDARN Inuvik and Rankin Inlet radars, respectively.

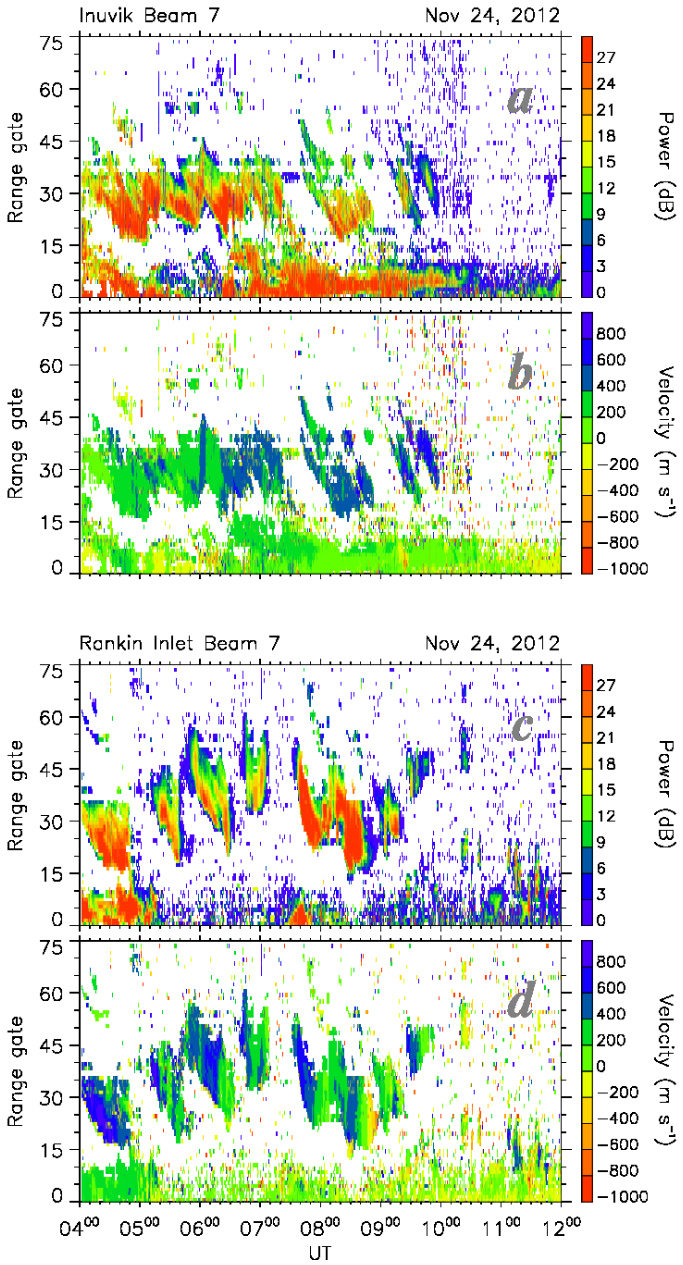

Figure 6 (a) Range-Time-Intensity (RTI) plot showing backscatter power along beam 7 of the SuperDARN Inuvik radar from 0400 to 1200 UT on 24 November 2012. (b) Range-Time-Intensity (RTI) plot showing the line-of-sight Doppler velocity along beam 7 of the SuperDARN Inuvik radar from 0400 to 1200 UT on 24 November 2012. (c) Same as (a), but using data from the SuperDARN Rankin Inlet radar. (d) Same as (b), but using data from the SuperDARN Rankin Inlet radar.